Measuring the effects of topically applied skin optical clearing agents and modeling the effects and consequences for laser therapies.

Wim Verkruysse [*,a], Misbah Khan[a], Bernard Choi[a], Lars O. Svaasand[b], Stuart J Nelson[a].
[a]Beckman Laser Institute and Medical Clinic, University of California, Irvine. CA 92612
[b]Norwegian University of Science & Technology, Department of Physical Electronics, N-7491 Trondheim, Norway

ABSTRACT

Human skin prepared with an optical clearing agent manifests reduced scattering as a result of de-hydration and refractive index matching. This has potentially large effects for laser therapies of several skin lesions such as port wine stain, hair removal and tattoo removal. With most topically applied clearing agents the clearing effect is limited because they penetrate poorly through the intact superficial skin layer (stratum corneum). Agent application modi other than topically are impractical and have limited the success of optical clearing in laser dermatology. In recent reports, however, a mixture of lipofylic and hydrofylic agents was shown to successfully penetrate through the intact stratum corneum layer which has raised new interest in this field. Immediately after application, the optical clearing effect is superficial and, as the agent diffuses through the skin, reduced scattering is manifested in deeper skin layers. For practical purposes as well as to maximize therapeutic success, it is important to quantify the reduced scattering as well as the trans-cutaneous transport dynamics of the agent. We determined the time and tissue depth resolved effects of optically cleared skin by inserting a microscopic reflector array in the skin. Depth dependent light intensity was measured by quantifying the signal of the reflector array with optical coherence tomography. A 1-dimensional mass diffusion model was used to estimate a trans-cutaneous transport diffusion constant for the clearing agent mixture. The results are used in Monte Carlo modeling to determine the optimal time of laser treatment after topical application of the optical clearing agent.

Keywords: scattering coefficient, treatment depth, reflector array, refractive index matching, topical application.

1. INTRODUCTION

Optical scattering in human skin is mainly due to refractive index differences between the various skin constituents such as water, collagen, intracellular components and ground substance. Optical scattering in human skin can greatly reduce image resolution and the depth of effective fluence for light based diagnostic methods and therapeutic applications, respectively. Optical clearing agents (OCA) have been shown to significantly reduce light scattering by refrasctive index matching [1-6]. OCA can be applied to the skin either topically or injected intra-dermally. With most topically applied OCA, the clearing effect is very limited because of minimal penetration through the intact stratum corneum. The limited penetration is due to the fact that Recently, however, we described an OCA mixture of lipophilic (polypropylene glycol based polymers or PPG) and hydrophilic (polyethylene glycol or PEG) substances that appears to induce optical clearing in human skin after topical application [7]. We will refer to this mixture as PPG:PEG in the following. The visibility of relatively deep structures increased significantly and the hypothesis that the OCA had indeed reduced optical scattering in the dermis was supported by *qualitative* interpretation of optical coherence tomography (OCT) images and cross-polarized photography. Subsequently, use of this OCA in conjunction with laser therapy led to enhanced fading of tattoo ink [8]. Since this mixture is relatively new, most of its properties regarding optical clearing and its trans-cutaneous diffusion dynamics have been determined qualitatively only.

To model optical clearing and maximize its clinical utility, it is important to *quantify* the reduced scattering and determine the percutaneous transport dynamics (diffusion constant) of OCA in human skin. For example, it is anticipated that the clearing agent progressively penetrates the skin. As a result, the optical clearing is stronger in the

* verkruw@laser.bli.uci.edu, phone 1 949 824 3754, fax 1 949 824 3754 www.bli.uci.edu

Optical Interactions with Tissue and Cells XVI, edited by Steven L. Jacques, William P. Roach, Proc. of SPIE Vol. 5695 (SPIE, Bellingham, WA, 2005)
1605-7422/05/$15 · doi: 10.1117/12.591421

superficial skin layers immediately after topical application and then gradually reaches deeper skin layers. The speed with which the agent diffuses through the skin layers has consequences for the timing of laser therapy. The objective of this study is twofold. First, quantify time and depth resolved optical clearing effects of the mixture in human skin. Second, use the results to investigate the consequences for laser therapy. More specifically, the optimal waiting period between topical application and laser will be studied using Monte Carlo simulations of laser light distributions in a port wine stain skin model.

Several optical techniques to quantify depth resolved scattering in human tissue already exists [4,9-15]. Most of these methods are accurate and have high spatial resolution. Unfortunately, however, the corresponding maximum measurement depths are limited (several hundreds of micrometers) or require a technique called focus tracking which can be time consuming. In addition, tissue reflectivity is usually assumed to be constant [14] or to have a constant relationship with scattering [12], which may not always be accurate. In the following we present results obtained with a new technique using OCT in combination with a microscopic reflector array, to estimate depth resolved light scattering coefficients after topical OCA application. OCT is a technique that uses optical interferometry of a broad band light source to non-invasively determine reflectance at discretely specified depths within a scattering medium such as biological tissue. While imaging is the most popular medical application of OCT, it is increasingly used to quantify tissue optical properties. Our new technique is an example of the latter application. In addition to quantification of the scattering coefficient, the measurements with the presented new technique allow for an estimate of the diffusion constant which describes the percutaneous transport dynamics of OCA in human skin.

2. METHODOLOGY

2.1 Quantification of Optical Clearing using a reflector array and optical coherence tomography

The amplitude of an OCT signal *A(z)* from a certain depth z in tissue depends mainly on three factors. First, the attenuation of the light by the overlying tissue. Second, the local reflectivity, or backscatter coefficient, *R(z)* of the tissue at depth z. Third, the sampling beam shape *I(z)* which depends on the numerical aperture of the sampling probe. The intensity of the sampling beam is highest in the focus of the sampling beam. When a low numerical aperture is used, however, the detection beam shape can be nearly collimated for the relevant depth of field and the effect of *I(z)* on *A(z)* can be minimized. For this paper we used a low numerical aperture (<0.1). Nevertheless, we measured the beam shape and implemented the effects of it in our analysis. The OCT signal *A(z)* can be approximated by equation 1:

$$A(z) \propto I(z)R(z)\exp(-\mu_t(z)\ z) \qquad (1)$$

where the total attenuation coefficient $\mu_t(z)$ equals the sum of the absorption coefficient $\mu_a(z)$ and the scattering coefficient $\mu_s(z)$. We will assume that $\mu_a(z)$ is negligible for the wavelength (λ = 1305 nm) and the tissue (human skin *ex vivo*) considered in our experiments. Moreover, in the following analysis we will also assume the effect of modified refractive index on the sampling beam shape *I(z)* to be negligible.

When a clearing agent is topically applied, the agent penetrates and dehydrates the skin and then matches the refractive index of the remaining collagen. As a result, not only the scattering coefficient $\mu_s(z)$ is reduced but the reflectivity *R(z)* as well. With this in mind it can be easily concluded from equation 1 that the signal *A(z)* can either go up or down when an optical clearing agent is applied, depending on the depth at which the OCT signal is measured and the depth at which the agent has penetrated. The effect of a reduced reflectivity *R(z)* may be compensated by a reduced scattering coefficient and a reduced attenuation. When OCT is used to quantify the effect of a clearing agent, one is confronted with the problem that there are *two* unknowns (*R(z)* and $\mu_s(z)$ (z)) while only *one* measurement is taken (A(z)). Our method aims at eliminating one unknown, *R(z)*, by inserting a reflector array in the skin tissue. The reflecting surfaces of the silicon array (refractive index $n_{Si} \approx 3.45$) provide a reflectivity in tissue that is virtually independent of the local OCA concentration. As a result the measured OCT signal (*A(z)*) can be used to determine the scattering coefficient $\mu_s(z)$.

Reflector arrays were fabricated out of silicon (refractive index $n_{Si} \approx 3.45$) using standard semiconductor fabrication techniques (Figure 1A). The designs were first patterned on a positive photo-resistant coated silicon wafer using a high resolution UV mask. Then, arrays were etched out from the silicon wafer using deep reactive ion etching after which a thorough cleansing process with acetone and iso-propanol removed any organic residue.

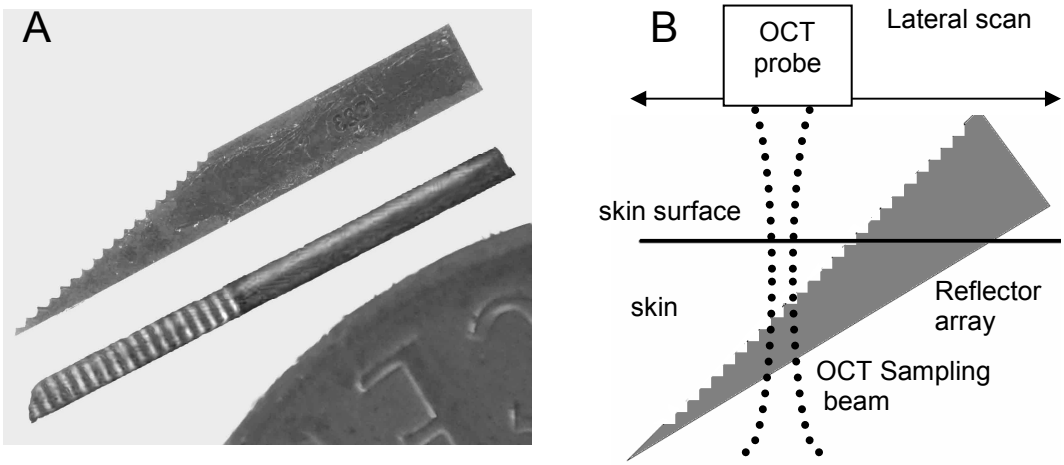

Figure 1. **A:** Fotograph of reflector array, side view and top view. The reflecting surfaces are 0.175 mm apart. A part of a penny is included for size comparison. **B:** Schematic drawing of the reflector array inserted in tissue and the scanning direction of the OCT probe along the surfaces of the reflector array.

We performed a series of experiments in which we inserted the reflector arrays with reflecting surfaces at distances of 0.175 mm in a piece of excised human skin, *ex vivo*. With a pair of tweezers, we inserted the arrays such that the reflecting flat surfaces were parallel to the skin surface (Figure 1B) and thus perpendicular to the OCT sampling beam to optimize the signal from these surfaces. We topically applied the OCA mixture PPG:PEG and started taking OCT measurements at regular time intervals. A second, identical, reflector array was inserted in a second piece of skin which served as a control to ensure that observed effects are the result of the OCA mixture only. On this control sample we used Surgilube^{Æ} (SL). SL is a skin surface refractive index matching agent that does not induce optical clearing in the dermis but remains at the most superficial skin layers. OCT measurements were of the reflector array in the skin samples were taken at regular intervals (1 minute intervals up to 10 minutes and 5 minutes up to 3 hours) on both skin samples. Alignment of the OCT probe with the reflector array typically took about 30 seconds. In between measurements, skin samples were kept in a 35 °C incubator to simulate the percutaneous transport dynamics of *in vivo* skin.

2.2 OCT image analysis and quantification of depth resolved scattering coefficient

The OCT measurements of the reflector arrays in the skin tissue provided us with images which were quantitatively analyzed as described in the following. Digital image analysis (pixel by pixel evaluation of $A_i(z)$) was used to determine the average (to remove the impact of speckle on the results) intensity $A_i(z_i)$ of each of the reflector surfaces at depths z_i. Because the skin tissue surfaces were not perfectly flat, we used digital image analysis to determine the depths z_i of each of the reflector surfaces with respect to the skin surface. At each time interval, we realigned the tissue sample with reflector probe four times and recorded for each re-alignment an OCT image to obtain an impression of the measurement error involved with this method. Each OCT image was analyzed separately and the results were averaged. Next, we plotted $A_i(z_i)$ versus z_i (for each reflecting surface i) providing us with curves of relative (OCT) light intensity versus tissue depth at different times after topical application of PPG:PEG or SL (control). Using a semi logarithmic scale, the slopes of these curves correspond to the total attenuation coefficient $\mu_t(z)$ (See equation 1). With our assumption that absorption is negligible at the OCT wavelength used, $\mu_t(z)$ equals the scattering coefficient $\mu_s(z)$. This analysis provides us with estimates of the depth resolved scattering coefficient $\mu_s(z)$ at each time interval.

2.3 Fitting the results with a transport diffusion model.

In an attempt to interpret the results in terms of trans-cutaneous transport dynamics, we assumed that the OCA concentration $C_{OCA}(t,z)$ can be described with a 1-dimensional diffusion transport model as in equation 2:

$$\frac{\partial C_{OCA}(t,z)}{\partial t} = D\frac{\partial^2 C_{OCA}(t,z)}{\partial z^2} \qquad (2),$$

in which D is the transport diffusion coefficient describing the mass transport of the OCA through the tissue, and *t* is the time after topical application of the OCA. A solution of equation 2 for a semi-infinite medium (the tissue samples) is:

$$C_{OCA}(t,z) = C_{OCA,sat}\,erfc\left(z/(2\sqrt{Dt}\right) \qquad (3),$$

where *erfc* is the complementary error function and $C_{\mathrm{OCA,sat}}$ is the maximum OCA concentration that is reached in tissue at saturation condition Figure 2A shows an example of OCA concentration depth profiles, predicted by the transport model (equation 3). For an interpretation of the $\mu_s(z)$ results in terms of this transport model, we have to assume a relationship between $\mu_s(t,z)$ and the OCA concentration $C_{\mathrm{OCA}}(t,z)$. Unfortunately, to our best knowledge this relationship is unknown. It seems reasonable, however, to assume that $\mu_s(t,z)$ decreases with increasing OCA concentration. An example of a hypothesized relationship is shown in Figure 2B. The maximum and minimum values of $\mu_s(t,z)$ for OCA concentrations equalling 0 and $C_{\mathrm{OCA,sat}}$, respectively are determined from our OCT measurements immediately, and hours after topical application of the OCA (see section 2.2). Combining Figures 2A and 2B, Figure 2C gives examples of modeled depth profiles of $\mu_s(z)$ at different times *t.* Finally, corresponding light intensities, computed with the depth dependent scattering (attenuation) coefficients of Figure 2C, are illustrated in Figure 2D. Model curves as in Figure 2D were used to fit on the measured curves (see section 2.2) to estimate the mass transport diffusion constant *D* in equations 2 and 3.

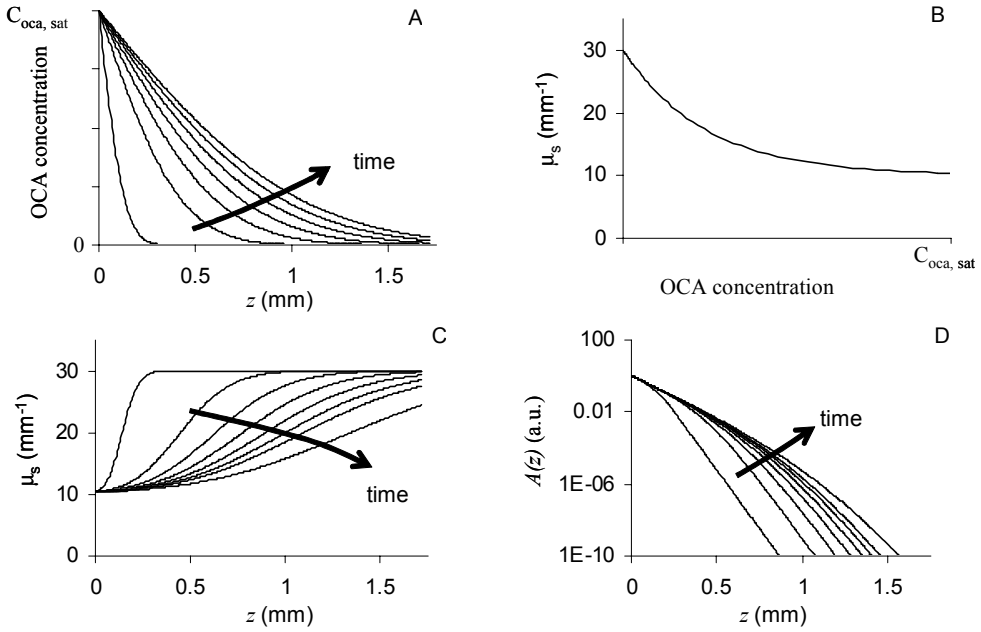

Figure 2. **A:** Examples of OCA concentration profiles as predicted by the mass transport diffusion mode for times t = 3, 30, 60, 90, 120, 150 and 180 minutes. B: An assumed relationship between the OCA concentration and the tissue scattering coefficient. C: Scattering coefficient profiles corresponding to the profiles in Figures A and B. D: The OCT amplitude profiles as computed with the scattering coefficient profiles in Figure C.

2.4 Transcutaneous transport dynamics of PPG:PEG used in a model of laser therapy

Many laser therapies in dermatology are based on the principle of selective photo-thermolysis [16]. In the laser treatment of Port Wine Stain (PWS), for example, the target chromophore is (oxy)hemoglobin in the erythrocytes in the ectatic

vasculature. Alternatively, in the laser treatment of tatoos, chromophores in the ink particles are targets for selective photo-absorption. In many of these therapies, melanin in the epidermis is a competing absorber. Heat production in the epidermis during a laser pulse and the associated risk on scarring are a limiting factor in terms of maximum radiant exposure of a laser pulse. In order to understand the consequences of PPG:PEG for a laser therap at we extrapolated the results we found in this study for the OCT wavelength of 1305nm to that of a typical laser therapeutic wavelength for PWS: 585 nm. In a simple simulation of a PWS laser treatment we assumed the same reduction in dermal scattering coefficient to occur at 585 nm than the reduction we estimated at 1305 nm. We emphasize that we do not have a sound theoretical nor experimental basis for this assumption. However, it seems plausible that the general trend is similar: a reduced scattering at 1305 nm, caused by refractive index matching agents is likely to coincide with a reduced scattering at 585 nm.

To simulate a PWS laser treatment we used a Monte Carlo algorithm to estimate light distributions and corresponding energy depositions in a multi layered semi-infinite medium (representing the skin) with discrete absorbing cylinders (representing ectatic vasculature of the PWS). The multiple dermal layers together simulate dermal scattering coefficient profiles similar to those depicted in Figure 2C. An illustration of the skin model is shown in figure 3

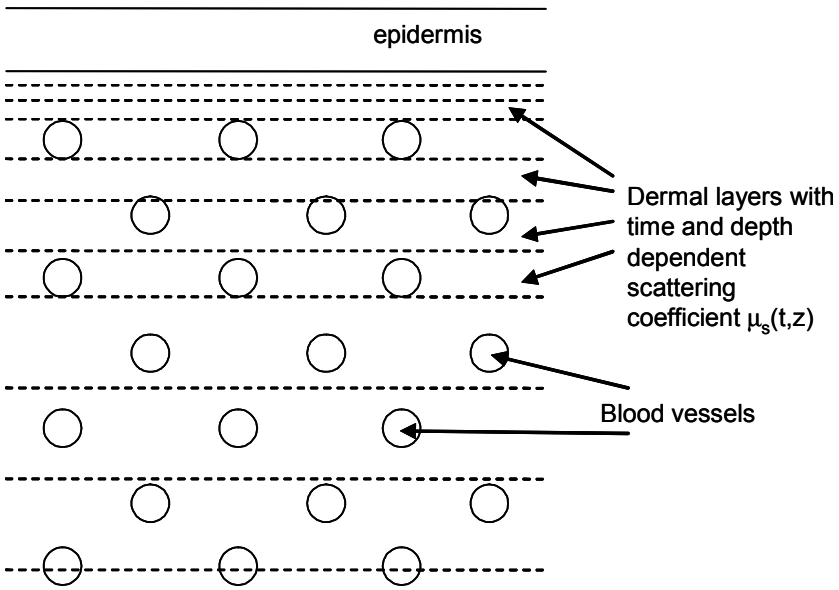

Figure 3: The port wine stain skin geometry used in Monte Carlo simulations of light and laser energy distributions during a therapeutic laser pulse. The dermis is modeled as a number of separate layers, each with dermal scattering coefficient determined by a mass transport diffusion model of OCA in skin and a relation ship of μs with the OCA concentration. Vessel radius in the skin model was 25 μm, which corresponds to a 5% dermal blood volume fraction. Epidermal thickness was 0.1 mm.

3. RESULTS

3.1 Quantification of Optical Clearing using a reflector array

A selection of OCT images of *ex vivo* human skin are shown in Figure 4 obtained before, immediately after, and 2 hours after application of either SL (Figures 4A-C) or the PPG:PEG mixture (Figures 4D-F). The highly scattering stratum corneum is visible as a dark thin layer at the skin surface in Figures 4A and 4D. Immediately after application of either SL or PPG:PEG (Figures 4B and 4E, respectively), both agents significantly reduced scattering in the stratum corneum. After 2 hours, the PPG:PEG mixture optically cleared the deeper dermis (Figure 4F). For the SL sample, the reduced scattering remains confined only to the stratum corneum (Figure 4C).

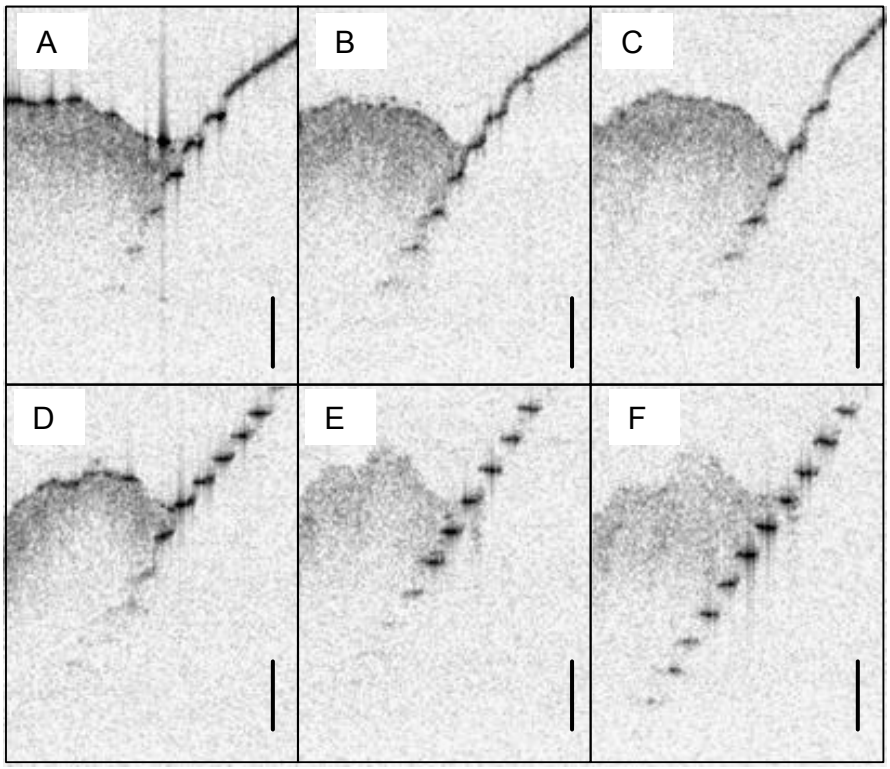

Figure 4: OCT images of the microscopic reflector arrays in ex vivo human skin. A) before, B) immediately after and C) 2 hours after topical application of SL. D) Before, E) immediately after, and F) 2 hours after topical application of the PPG:PEG mixture. Scale bar = 0.5 mm.3.2 OCT image analysis and quantification of depth resolved scattering coefficient

OCT signal amplitudes, $A(z)$, from images taken at t = 1, 25, 70 and 190 minutes after topical application of SL and PPG:PEG, versus tissue depth z, are shown in Figure 5. For SL, (Figure 5A) the curves are more or less straight for z up to approximately 1.25 mm, indicating a constant value for $\mu_s(z)$. For deeper z, $A(z)$ is dominated by noise rather than the reflected signal from the array.

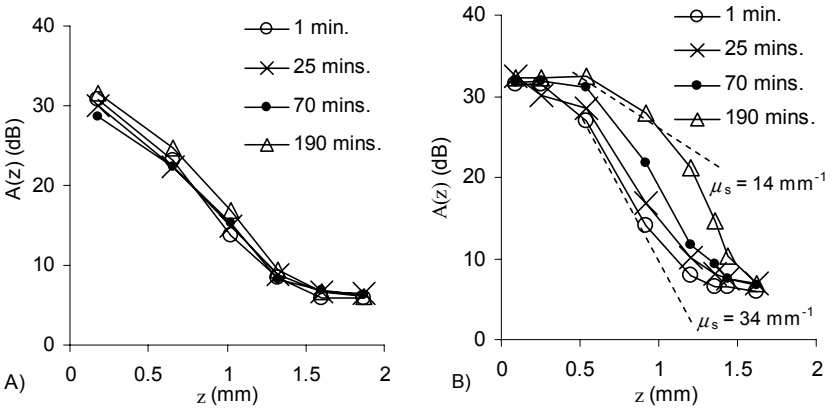

Figure 5: Peak amplitudes A(z) at the reflector surfaces plotted versus tissue depth z. Curves are for different times after topical application of either SL (A) or the PPG:PEG mixture (B). Dashed lines, representing reduced tissue optical scattering as indicated by μ_s, are included in B) for comparison with the measured data.

The lack of appreciably improved visibility for the reflectors in the SL sample (Figures4 and 4C) is in agreement with the fact that the curves for different times in Figure 5A are all very similar to one another. This is in sharp contrast to the curves shown in Figure 5B for the PPG:PEG mixture. The improved visibility of the deeper reflectors in Figure 4F is confirmed by the higher relative $A(z)$ and thus a lower attenuation, shown in Figure 4B. Note that the slope of the curves in Figure 5B remains relatively steep for deeper z until $A(z)$ reaches the background noise level at which point the slopes flatten out. The reduced attenuation over time corresponds to the fact that the PPG:PEG mixture diffuses into the skin and optically clears the epidermis and upper dermis. The relative intensities at the first 3 reflectors are somewhat unexpected; the intensities are not reduced with z and sometimes even increase with z which can not be fully explained. Therefore, to determine values for μ_s, we only used the relative light intensities from 0.5 to 1.25 mm. Immediately after topical application of either SL or the PPG:PEG mixture, the resulting values for μ_s are 22 and 34 mm^{-1}, respectively. After 2 hours, μ_s remains 22 mm^{-1} in the SL sample while μ_s was reduced from 34 to 14 mm^{-1} for the PPG:PEG mixture (dashed lines in Figure 5B). Values for μ_s at depths shallower than 0.5 mm are even smaller than 14 mm^{-1} but hard to quantify accurately with the current data.

3.2 Fitting the results with a transport diffusion model.

We have used the model described in section 2.3 as well as the relationship between C_{OCA} and μ_s depicted in Figure 2B, to fit the measured data of Figure 5B on curves, described by this model. The relationship between c(z,t) andμ_s. is unknown, yet we found that the results of the above described model are very sensitive to changes in the diffusion constant, D, more sensitive than for changes in the assumed relationship between C_{OCA} and μ_s. Hence, the fit of the model to the measured curves allows for a relatively robust estimate of the order of magnitude for D. We tested a variety of relationships between C_{OCA} and μ_s. (linear as well as the exponential one shown in figure 2B), each describing a decrease in μ_s. for an increase in c(z,t). Based on the ranges of estimated model parameters, we estimate values for D to be 5x10-8 - 5x10-7 cm^2/s.

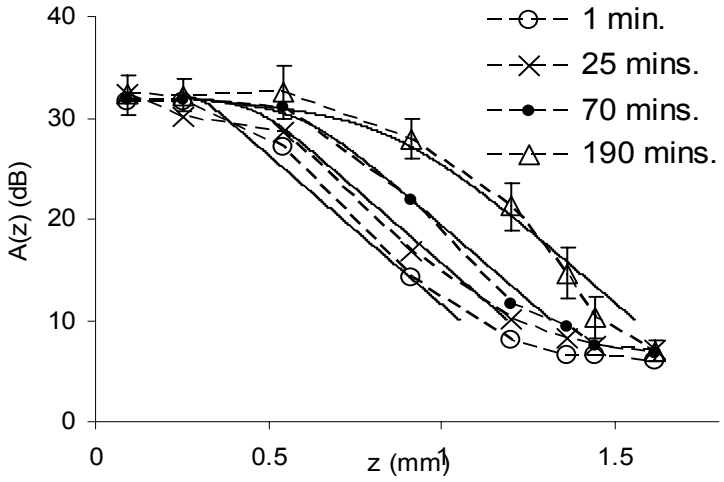

Figure 6 Measured curves (dashed lines), also shown in 5B, are compared with calculated curves (solid lines) based on a simple mass diffusion model. The diffusion constant used is $6x10^{-8}$ cm^2/s. Error bars (representing the standard deviation of results from 4 OCT images) are shown for one curve only, for reasons of clarity.

3.3 Trans-cutaneous transport dynamics of PPG:PEG used in a model of laser therapy.

The profiles were computed with Monte Carlo and the skin model depicted in Figure 3. Dermal scattering properties were chosen to simulate a laser pulse at 585 nm [17], a commonly used wavelength for port wine stain laser therapy. The impact of OCA on dermal scattering was modeled by assuming the same dependency on OCA concentration as illustrated in Figure 2B.

The curves in Figure 7 illustrates how light distributions (A) and deposited energy profiles (B-D) are affected by optical clearing and what time periods are involved for the effects to occur. The profiles are for different times after topical application of PPG:PEG. It is well known that when tissue is irradiated with collimated laser light, the light fluence in tissue can be higher than the incident fluence. In Figure 7A, the small horizontal line at 1 indicates the incident fluence, thus illustrating that the subsurface fluences are up to 2.5 times higher than the incident fluence. This effect is undesired in some treatments because, as said, light absorption in epidermal melanin is associated with a risk on scarring. Figure 7A also shows that this effect is strongly reduced even only several minutes after topical application of PPG:PEG. Obviously, this is an immediate result of the reduced scattering coefficient in the most superficial skin layers. For longer time periods after application (Figures 7C and D), the subsurface fluence continues to decrease somewhat but the most significant differences between optically uncleared and cleared skin are noticed at larger depths. The deposited energy in vasculature is increased significantly when a laser pulse is applied at some time (e.g. > 30 mins) after topical application of the OCA. The progressive penetration of the OCA reduces the dermal scattering coefficient for larger parts of the dermis and causes the attenuation of laser light due to scattering to be reduced.

To estimate a maximum depth of vascular injury without epidermal thermal damage for each time period after topical OCA application, we use the same damage criterion we used in an earlier study [17]. This criterion states that the maximum depth of vascular injury is the depth at which a vessel receives the same amount of deposited energy (and consequent heat production) as the epidermis. The maximum depths of vascular injury are indicated by horizontal dashed lines in Figures 7 B, C and D. In addition, we also use arrows to illustrate the increased depth of vascular injury between optically uncleared skin (dashed arrow) and optically cleared skin (solid arrows).

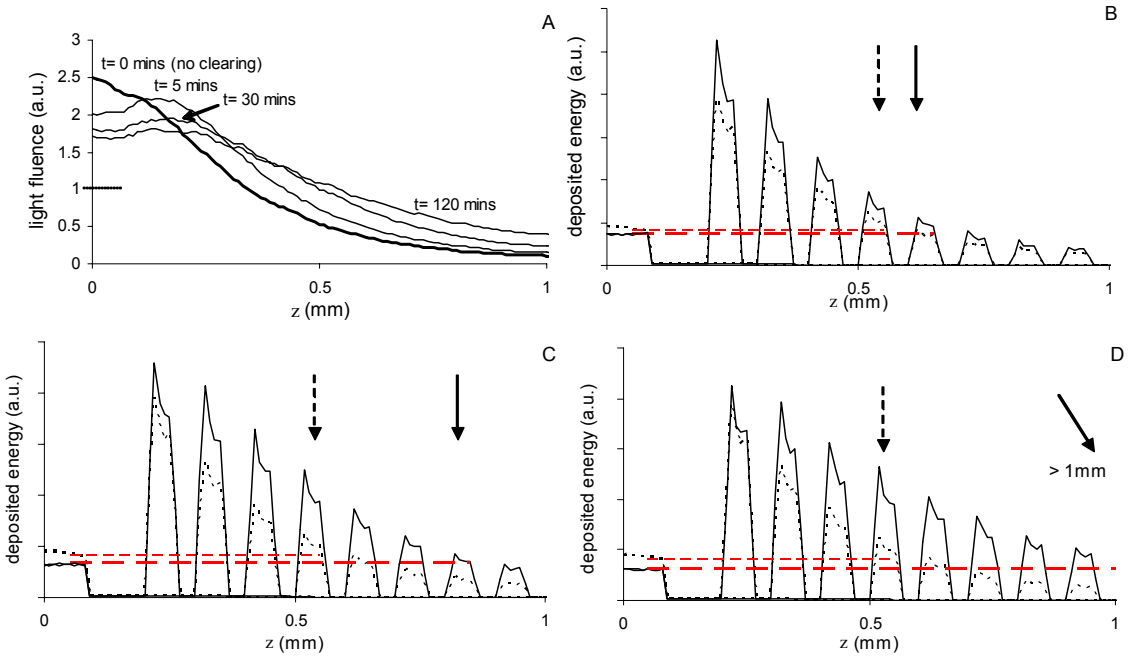

Figure 7 A: Light fluence profiles computed with Monte Carlo for different times (t =0, 5, 30 and 120 mins) after topical application of PPG:PEG using the mass transport diffusion model. B,C and D: Corresponding depth profiles of the deposited laser energy in epidermis and vessels. In each figure the uncleared deposited energy profile is compared with the profiles for either t =5, 30 or 120 mins in Figures B, C and D, respetively. The value for D (6×10^{-8} cm^2/s) and dermal scattering coefficients for uncleared and completely cleared (μ_s = 30 and 10 mm^{-1}, respectively) are estimated from the OCT/reflector array measurements.

4. DISCUSSION

The μ_s values for human skin (22 and 34 mm^{-1}) determined for human skin are close to those previously reported by Du et al, [18]at the OCT probe wavelength of 1305 nm for porcine skin in vitro (22 27 mm^{-1}), using a double integrating sphere method. However, they are somewhat higher than values measured by Kn¸ttel et al. [12] for in vivo human skin (2 ñ 10 mm^{-1}) using OCT.

The accuracy of our current data does not allow for a precise description of the percutaneous dynamics of the OCA through the epidermis and upper dermis. However, a 1-dimensional diffusion model (Equation 3), describing mass transport of the OCA in human skin, combined with a relationship between the concentration c(z,t) and describes the overall effects observed in Figure 4B reasonably well (Figure 5).

Based on the ranges of estimated model parameters, we estimate values for D to be $5x10^{-8}$ - $5x10^{-7}$ cm^2/s. These values are noticeably smaller (by approximately 2 orders of magnitude) than those reported by Tuchin et al. [14] which can be explained by the fact that the molecules those authors studied are much smaller than those in the PPG:PEG mixture and, therefore, diffuse faster. Preliminary experiments using our method (not presented here) indicate that a 1:2 ratio of PPG:PEG diffuses faster than the 1:1 ratio used in this study.

The described application of OCT to quantify scattering optical properties of human skin is distinctly different from previously proposed methods using OCT [12,13,19,20]. The latter methods are generally based on focus tracking (also referred to as dynamic focusing). In this approach, the OCT measurement involves, in addition to the regular lateral and axial scans to form a 2-D image, an additional scan of the sampling beam optical focus around each pixel at each sampling depth. Variation in the OCT signal resulting from the latter scan provides *localized* optical scattering properties at each sample depth. In contrast, our method determines average *bulk* attenuation of light with depth between two array reflectors by comparing the corresponding intensities. The relative usefulness of either approach may depend on the purpose of the investigation. To study local tissue optical scattering at high spatial resolution, the focus tracking methods are obviously preferential. For dosimetry purposes to optimize laser therapies, bulk attenuation of light over relatively large tissue depths, as measured with the presented method are a more direct and useful measure. Refinement of our method to increase accuracy, however, is warranted and currently undertaken at our institute.

Several other differences between the array method and focus tracking methods should be mentioned. First, in contrast to the latter methods, the former method is invasive, albeit minimal. Second, the array method does not require a specialized OCT system with dynamic focusing capabilities. Third, the focus tracking methods implicitly assume a constant relationship of $R(z)$ with $\mu_s.(z)$[12,21] which may not necessarily be accurate in the case of optically cleared human skin . Finally, a noteworthy advantage of our method is that despite the very low NA, signals at z greater than 1mm are still well above the background noise level. The high reflectivity of the array (compared to that of skin structures) compensates for the low light intensity in the OCT sample beam and increases the effective dynamic range and depth of the OCT measurement. This may be of particular importance in the optimization of OC for clinical applications where the target is relatively deep (> 1mm) such as in removal of tattoos [8] or hair.

It should be emphasized that the study of light distributions calculated with Monte Carlo are shown with the underlying assumption that dermal scattering at 585 nm shows similar behavior than at 1305 nm when exposed to PPG:PEG. As mentioned, depending on the geometry, dermal scattering can both increase and decrease local light fluence. Therefore, it was not a priori clear if it is beneficial to wait with a laser pulse until the OCA has penetrated even the deepest skin layers. It is interesting to note that our simple analysis suggests that there is no optimal period between application of the OCA and the laser pulse. It also suggests that after some 30 minutes or longer, most of the anticipated beneficial effects on the laser therapy are obtained.

5 Conclusion

To our knowledge, this study is the first to quantify optical clearing and percutaneous transport dynamics of a topically applied OCA in general, and the PPG:PEG mixture in particular. The results confirm that the topically applied PPG:PEG mixture penetrates through the intact stratum corneum and subsequently optically clears deeper skin layers. Moreover, the use of a reflector array in OCT to estimate $\mu_s(z)$ is, we believe, a novel method.

Acknowledgments: This work was supported by the following grants from the National Institute of Health (AR47551, AR48458 and EB002495) and the Arnold and Mabel Beckman Fellows program (BC). We kindly thank Dr. Shu-Guang Guo and Dr. Zhongping Chen for advice and assistance with the OCT measurements.

REFERENCES

[1] R. K. Wang and V. V. Tuchin. Tissue clearing as a tool to enhance imaging capability for optical coherence tomography. SPIE **4619**, 22 (2002).
[2] G. Vargas. Reduction of light scattering in biological tissue: Implications for optical diagnostics and therapeutics, *Biomedical Engineering*, The University of Texas at Austin, Austin, TX, 2001.
[3] G. Vargas, E. K. Chan, J. K. Barton, H. G. Rylander, and A. J. Welch. Use of an agent to reduce scattering in skin. Lasers Surg. Med. **24**, 133 (1999).
[4] V. Tuchin, I. Maksimova, D. Zimnyakov, I. Kon, A. Mavlutov, and A. Mishin. Light propagation in tissues with controlled optical properties. J Biomed Opt **2**, 401 (1997).
[5] A. T. Yeh, B. Choi, J. S. Nelson, and B. J. Tromberg. Reversible dissociation of collagen in tissues. J. Invest. Dermatol. **121**, 1332 (2003).
[6] R. K. K. Wang, X. Q. Xu, Y. H. He, and J. B. Elder. Investigation of optical clearing of gastric tissue immersed with hyperosmotic agents. IEEE Journal of Selected Topics in Quantum Electronics **9**, 234 (2003).
[7] M. Khan, B. Choi, S. Chess, K. M. Kelly, J. McCullough, and J. S. Nelson. Optical clearing of in vivo human skin: Implications for light-based diagnostic imaging and therapeutics. Lasers Surg. Med. **34**, 83 (2004).
[8] M. Khan, S. Chess, B. Choi, K. M. Kelly, and J. S. Nelson. Can topically applied optical clearing agents increase the epidermal damage threshold and enhance therapeutic efficacy? Lasers Surg. Med. **35**, 93 (2004).
[9] M. Kohl, M. Cope, M. Essenpreis, and D. Boecker. Influence of glucose concentration on light scattering in tissue-simulating phantoms. Opt. Lett. **19**, 2170 (1994).
[10] J. S. Maier, S. A. Walker, S. Fantini, M. A. Franceschi, and E. Gratton. Possible correlation between blood glucose concentration and the reduced scattering coefficient of tissues in the near infrared. Opt. Lett. **19**, 2062 (1994).
[11] A. N. Bashkatov, E. A. Genina, Y. P. Sinichkin, V. I. Kochubey, N. A. Lakodina, and V. V. Tuchin. Glucose and Mannitol Diffusion in Human Dura Mater. Biophys J **85**, 3310 (2003).
[12] A. Kn¸ttel and M. Boehlau-Godau. Spatially confined and temporally resolved refractive index and scattering evaluation in human skin performed with optical coherence tomography. J. Biomed. Opt. **5**, 83 (2000).
[13] A. Kn¸ttel, S. Bonev, and W. Knaak. New method for evaluation of in vivo scattering and refractive index properties obtained with optical coherence tomography. J. Biomed. Opt. **9**, 265 (2004).
[14] V. Tuchin, X. Xu, and R. Wang. Dynamic optical coherence tomography in studies of optical clearing, sedimentation, and aggregation of immersed blood. Appl Optics **41**, 258 (2002).
[15] G. N. Stamatas, J. Wu, and N. Kollias. Non-invasive method for quantitative evaluation of exogenous compound deposition on skin. J. Invest. Dermatol. **118**, 295 (2002).
[16] R. Anderson and J. Parrish. Microvasculature can be selectively damaged using dye lasers: A basic theory and experimental evidence in human skin. Lasers Surg Med **1**, 263 (1981).
[17] W. Verkruysse, J. W. Pickering, J. F. Beek, M. Keijzer, and M. J. C. van Gemert. Modeling the effect of wavelength on the pulsed dye laser treatment of port wine stains. Appl. Opt. **32**, 393 (1993).
[18] Y. Du, X. H. Hu, M. Cariveau, X. Ma, K. G. W, and J. Q. Lu. Optical properties of porcine skin dermis between 900 nm and 1500 nm. Phys Med Biol **46**, 167 (2001).
[19] G. J. Tearney, M. E. Brezinski, J. F. Southern, B. E. Bouma, M. R. Hee, and J. G. Fujimoto. Determination of the refractive index of highly scattering human tissue by optical coherence tomography. Opt. Lett. **20**, 2258 (1995).
[20] D. J. Faber, F. J. van der Meer, M. C. G. Aalders, and T. G. van Leeuwen. Quantitative measurement of attenuation coefficients of weakly scattering media using optical coherence tomography. Opt Express **12**, 4353 (2004).
[21] J. D. Klett. Stable analytical inversion solution for processing lidar returns. Appl. Opt. **20**, 211 (1981).